Available online at www.sciencedirect.com
ScienceDirect
Cement and Concrete Research 38 (2008) 803–815
Cement and Concrete Research

Influence of chemical and physical characteristics of cement kiln dusts (CKDs) on their hydration behavior and potential suitability for soil stabilization

Sulapha Peethamparan [a,b], Jan Olek [b,*], Janet Lovell [c]

[a] Department of Civil and Environmental Engineering, Princeton University, Princeton, NJ 08544, USA
[b] School of Civil Engineering, Purdue University, 550 Stadium Mall Drive, West Lafayette, IN. 47907-2051, USA
[c] Charles Pankow Concrete Materials Laboratory, Purdue University, 550 Stadium Mall Drive, West Lafayette, IN. 47907-2051, USA

Received 29 December 2006; accepted 23 January 2008

Abstract

The interaction of CKDs with a given soil depends on the chemical and physical characteristics of the CKDs. Hence, the characterization of CKDs and their hydration products may lead to better understanding of their suitability as soil stabilizers. In the present article, four different CKD powders are characterized and their hydration products are evaluated. A detailed chemical (X-ray diffraction), thermogravimetric and morphological (scanning electron microscope) analyses of both the CKD powders and the hydrated CKD pastes are presented. In general, high free-lime content (~14–29%) CKDs, when reacted with water produced significant amounts of calcium hydroxide, ettringite and syngenite. These CKDs also developed higher unconfined compressive strength and higher temperature of hydration compared to CKDs with lower amounts of free-lime. An attempt was made to qualitatively correlate the performance of CKD pastes with the chemical and physical characteristics of the original CKD powders and to determine their potential suitability as soil stabilizers. To that effect a limited unconfined compressive strength testing of CKD-treated kaolinite clays was performed. The results of this study suggest that both the compressive strength and the temperature of hydration of the CKD paste can give early indications of the suitability of particular CKD for soil stabilization.

Keywords: Cement kiln dust; Characterization; X-ray diffraction; SEM; Thermal analysis

1. Introduction

Cement kiln dusts (CKDs) are finely divided, dry particulate materials carried out from a cement kiln by exhaust gases, and captured by the kiln's air pollution control system. Recent technological advances in the cement production process have resulted in substantial reduction in the quantities of CKDs generated per ton of cement. Nonetheless, in most cement plants, disposal of CKDs is a substantial economical and environmental problem. An estimate of the amount of CKDs generated and land filled every year in the United States is presented in the Federal Highway Administration report [1]. Approximately 14.2 million tons of CKDs are generated and 64% of this amount is re-used within the cement plants themselves as raw feed material. The remaining 36% is considered to be an industrial waste, and only 6% of it is currently used in miscellanies applications. That leaves 4.3 million tons of CKDs to be stockpiled or deposited in land fills. Exploring ways to make use of CKDs as a value-added product has been of great concern, since achieving further reduction in their generation will become increasingly difficult due to technical issues related to efficiency of cement production process.

In general, CKDs are mixtures of airborne particles of cement raw materials, partly processed cement components, and volatile components condensed on their surfaces. They vary in

* Corresponding author.
E-mail addresses: speetham@princeton.edu, peethamp@purdue.edu (S. Peethamparan), olek@purdue.edu (J. Olek), lovell@purdue.edu (J. Lovell).

0008-8846/$ - see front matter © 2008 Elsevier Ltd. All rights reserved.
doi:10.1016/j.cemconres.2008.01.011

composition, but most of them contain silica, calcium carbonate, and calcium oxide ("free lime"); many also contain alkali sulfates and chlorides and sometimes other minor components. The proportions of various compounds are highly variable. Most CKDs tend to generate relatively high pH levels when mixed with water. The higher alkalinity and finer particle size, in addition to their (sometimes) cementitious properties, make these materials usable for several applications: waste solidification [2,3], replacement of portland cement in concrete block manufacturing and ready mix concrete [4–11], construction of hydraulic barriers in a landfill liner/cover applications [12], use as agricultural soil amendments [13], flowable fills [14,15], and mineral fillers in asphalt paving and mine reclamation operations. The presence of free-lime (CaO), the high alkali content, and the high fineness of CKDs also make them potentially valuable materials for stabilizing soils [16].

Previous studies [17–19] have shown that treating soil with CKD can improve a number of its properties, and that some CKDs may be effective soil stabilizers. In one study [20], the unconfined compressive strength of 28 day old compacted kaolinite samples increased from 210 to 1115 kPa by addition of 16% (by weight) of a CKD. The addition of 8% of the same CKD resulted in a reduction of the plasticity index (PI) from 513 to 326% for highly plastic bentonite (Na-montmorillonite) clay. Greater reductions in PI were found with increased CKD content. Increased strength due to the addition of CKD was also reported for dune sands, with larger strength increases corresponding to higher percentage addition of CKD and longer curing periods [21]. Stabilization of highly expansive clay is, in particular, an area of major interest to the construction community due to the excessive swelling and shrinking experienced by this clay upon changes in moisture content. An existing study [18] has shown that CKD addition to a Na-montmorillonite clay resulted in 150% increase in the 28 day compressive strength (unsoaked) and 18% reduction in the plasticity index (PI) in 2 h after mixing compared to the untreated clay.

Hydrated lime ($Ca(OH)_2$) is the most commonly used soil stabilizer which, by reacting with clay (pozzolanic reaction) increases soils' stability [22,23]. Since some CKDs contain considerable amounts of free-lime, a similar stabilization mechanism might also be expected to occur in the CKD-treated soils. Being relatively complex, when reacting with water, CKDs may also produce other hydration products. These hydration products may significantly affect CKDs' soil stabilization potential. In particular, the alkalis and sulfates present in the CKDs may also play a significant role in the soil stabilization process by forming ettringite and syngenite in the hydrated CKD. For these reasons, it is important to characterize the CKDs and their hydration products, as that may lead to better understanding of the CKD-soil stabilization mechanisms.

The objective of the present study was to characterize different CKDs in order to qualitatively evaluate and compare the influence of the chemical and physical properties of these materials on their hydration behavior and potential suitability as soil stabilizers. This information might also provide some early indication of the expected durability of CKD-treated soil systems. The knowledge of the characteristics of CKDs and their hydration products might also be useful when trying to distinguish the reaction products formed in CKD-treated clay systems from those resulting from hydration of CKDs alone. In the present study, four different types of CKDs were used. These were selected to represent a range of chemical compositions (free lime, alkalies and sulfate contents) and physical (fineness) properties of the larger (17) suite of CKDs available from four cement producers. The characterization process of CKDs presented in this paper included physical analysis of CKD powder (particle size distribution and specific surface area), the chemical analysis (X-Ray fluorescence spectroscopy (XRF), XRD and TGA) and morphological analysis (SEM) of both the unhydrated CKD powder and the hydrated CKD-water pastes.

In addition, the temperature of hydration of the CKD pastes as well as their strength were also evaluated. Finally, the strength of the CKD-treated kaolinite was also obtained compared with the strength values of hydrated CKD-only paste in an attempt to assess how characteristics of CKDs influence their potential for clay stabilization. However, it is important to note that the suitability of CKD as potential soil stabilizer in the field depends on several factors other than strength and heat of hydration (e.g., clay content, local moisture conditions).

2. Material selection

Four different types of CKDs (from now on referred to as CKD-1, CKD-2, CKD-3 and CKD-4) were selected for the study, each from a different cement plant. Table 1 summarizes the details of the origins of the CKDs, including the type of processing technique, type of the kiln and information about raw materials used in the cement manufacturing processes. All CKDs were collected fresh at the cement plants, packed in plastic bags and stored in air tight plastic buckets. The X-ray and thermogravimetric analyses performed at various times during this study confirmed that there were no significant changes in chemical composition of CKDs during the storage period. The chemical composition of these CKDs was determined by X-ray fluorescence (XRF) spectroscopy and is shown in Table 2. For comparative purposes, chemical composition of a typical Type I portland cement is also included in this table. Similar to Type I portland cement, all CKDs contained significant amounts of calcium oxide (CaO), silicon dioxide (SiO_2), alumina (Al_2O_3) and ferric oxide (Fe_2O_3). However, the sulfur trioxide (SO_3) and alkali (K_2O and Na_2O) contents were significantly higher in CKDs compared to cement. The unreacted CaO (or free-lime), which is expected to play a major role in the soil stabilization, was highest in CKD-2 (29.14%) followed by CKD-1 (13.85%). The free-lime content in the remaining two CKDs was relatively low with 5.32% in CKD-3 and 3.26% in CKD-4.

The particle size distributions of the CKDs, determined using a laser particle size analyzer, are shown in Fig. 1. For comparative purposes, the particle size distribution of a typical Type I portland cement is also shown in Fig. 1. As per the

Table 1
The origins of CKDs used in the study

CKD	Processing technique	Type of kiln	Raw materials used in the cement manufacturing process
1	Dry	Long	Limestone, shale, sand and iron ore
2	Dry with precalciner	Short	Limestone, clay, bottom ash/fly ash, foundry sand/sludge, iron waste
3	Dry with pre-heater	Long	Limestone, clay, bottom ash and iron scale
4	Wet	Long	Limestone, clay, sand, fly ash and blast furnace slag

particle size distribution curves, the CKD-2 and CKD-1 had the finest and coarsest particle size distributions respectively. The other two CKDs (CKD-3 and CKD-4) had particle size distributions very similar to that of the Type I portland cement. The surface areas of the CKDs, as measured by the nitrogen BET method, were 2.6, 1.8, 2.4 and 2.8 m^2/g, respectively, for CKD-1, 2, 3, and 4. It can be seen that CKD-4 and CKD-2 had the highest and the lowest surface areas respectively. The discrepancy in relative CKD particle sizes indicated by particle size distribution and surface area measurements might be the result of both the differences in the degree of flocculation as well as in the internal porosity of CKDs.

The clay used was a commercial kaolinite clay, marketed as EPK® Pulverized Kaolin by the Fieldspar Corporation. The chemical composition of this clay is given in Table 2 and its surface area was measured as 27 m^2/g using nitrogen BET.

3. Sample preparation and experimental details

This section contains details regarding the preparation of test specimens and description of the test methods used for their characterization. In addition to powder chemical analysis techniques mentioned in Section 2, several analytical methods were used to further characterize the CKD powders and their hydration products. Additional techniques used during this research program include X-ray diffractometry, thermal analysis, scanning electron microscopy and energy dispersive X-ray spectrometry (EDX).

Table 2
Chemical composition of the materials used

Chemical composition by XRF	CKD-1	CKD-2	CKD-3	CKD-4	Type I cement	Kaolinite clay
	Weight (%)					
SiO_2	12.18	16.42	11.91	15.39	20.48	45.73
Al_2O_3	4.24	3.62	2.17	4.66	4.21	37.36
TiO_2	0.22	0.23	0.15	0.57	0.36	–
P_2O_5	0.08	0.09	0.09	0.09	0.09	–
Fe_2O_3	1.71	2.31	2.08	2.34	2.41	0.79
CaO	46.24	55.00	46.05	37.35	63.19	0.18
MgO	1.24	2.68	2.2	2.10	4	0.098
Na_2O	0.51	0.17	0.33	0.81	0.19	0.059
K_2O	4.89	2.89	1.43	7.0	0.28	0.33
Na_2O equiv.	3.72	2.05	1.27	5.36	0.37	–
Mn_2O_3	0.05	0.44	0.04	0.07	0.14	–
SrO	0.04	0.03	0.07	0.02	0.04	–
SO_3	14.62	12.69	4.21	5.80	2.76	–
Cl	0.59	0.74	0.35	3.26	–	–
LOI@ 750	14.22	3.92	29.63	27.65	1.76	–
Free CaO **	13.85	29.14	5.32	3.26	1.58	–
Water-soluble Na_2O *	0.28	0.06	0.12	0.59	0.04	–
Water-soluble K_2O *	2.95	1.68	0.93	6.33	0.16	–

**chemical analysis, *photo flame method.

3.1. Sample preparation

For CKD powder sample characterization, the "as received" CKD powders were used. For hydrated CKD characterization, the samples were prepared as follows.

The basic form of specimens studied in this work were small compacted cylinders, 33 mm in diameter and 71 mm in height, prepared using the Harvard miniature compaction apparatus [24]. This device uses a compaction method that closely duplicates the kneading action of the sheep's-foot roller used in field soil compaction, but requires only about 200 g of moist soil or soil mixtures. In preparation of the samples, each CKD was mixed with required amount of de-ionized water to bring the dry CKD powder to the designated 31% (by weight of dry sample) moisture content. The moistened powders were then compacted into the steel molds in four layers and each layer was compacted by applying 20 blows using an 18.14 (40 lb) hammer. The compacted cylinders were extracted immediately after compaction, wrapped in plastic bags, and placed in sealed plastic boxes stored in a room kept at 100% RH at a constant temperature of 23 °C. After designated curing periods of 1, 7 and 28 days, small (10 mm) cubic specimens were cut from the cylinders and soaked in acetone for 2 days to stop the hydration and subsequently dried in room temperature. Powder specimens for XRD and TGA analyses were prepared after grinding small portions of the dried specimens and sieving the ground material through a 200-mesh sieve. For strength tests, the 33 mm × 71 mm size cylinders were tested directly without any further treatment.

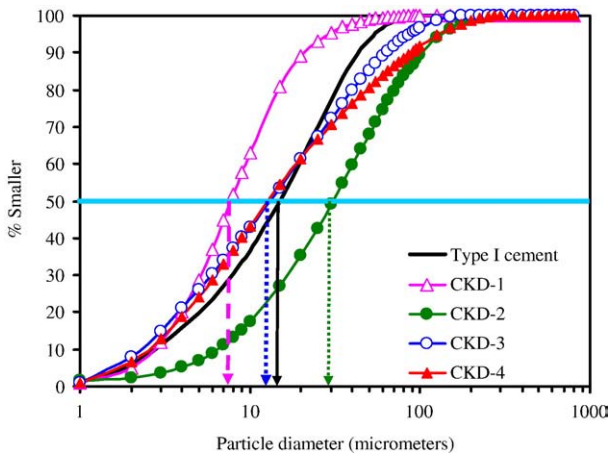

Fig. 1. Particle size distribution and the calculated specific surface areas of the CKD powders.

3.2. X-ray diffraction analyses

A Siemens D-500 diffractometer was used to perform X-ray diffraction analyses. The source of radiation used was CuKα with the tube powered to 50 kV at 30 mA. The random powder mount specimens prepared using the as received CKD powders and hydrated CKD powders prepared as per Section 3.1 were scanned from 3 to 65° 2-theta at 0.02° step size. The interpretation of the X-ray pattern for the presence of crystalline components was carried out by usual methods, involving assignment of each of the peaks present in the X-ray pattern to one (sometimes more than one) of the potential crystalline phases.

3.3. Thermogravimetric analyses

Thermogravimetric analyses (TGA) was performed using a TA 2950 thermogravimetric analyzer. Both, the CKD powder and the ground-up hydrated CKD specimens were tested. The hydrated samples were prepared as discussed previously in Section 3.1. In each case, the test sample weight used was 30± 0.5 mg. The sample was continuously heated from room temperature to 1000 °C in a nitrogen environment at a heating rate of 10 °C/min. Both TGA and differential TGA (DTGA) patterns were obtained.

3.4. Scanning electron microscopy

The morphologies of the CKD powders and their hydration products were examined using SEM. The particulate samples (CKD powder as received from the plant) were sprinkled onto double sided Scotch® tape. The small size cubic specimens prepared as described earlier (in Section 3.1) were fractured to reveal a clean fracture surface and mounted on aluminum stubs using carbon tape and silver paint. The samples were coated with platinum. They were then imaged in the secondary mode using high-resolution setting followed by EDX analysis. Imaging was performed using an FEI NOVA nanoSEM field emission scanning electron microscope utilizing either the ET (Everhart-Thornley) or TLD (Through-the-Lens) detector. The EDX was performed using an Oxford INCA 250 system using an accelerating voltage of 15 kV.

3.5. Temperature of hydration

The temperature of hydration of CKD pastes prepared at a moisture content of 31% was measured under quasi-adiabatic conditions. The samples of CKD alone or that of kaolinite clay mixed with 25% of CKDs were combined with required amount of de-ionized water and mixed according to ASTM C 150 [25] using a Hobart mixer. After mixing, the paste was cast into the 20 oz capacity thermoplastic containers with air tight lids. To prevent excessive heat losses, the container with the paste and temperature probe was placed in an insulated box. A thermocouple probe inserted into the mold recorded the temperature during hydration. The temperature was monitored over a period of 4 days.

3.6. Unconfined compressive strength

The compacted cylinders prepared using the procedure described in Section 3.1 were used for determining the unconfined compressive strength (UCS). Two sets of samples were prepared, consisting of (1) CKD alone samples and (2) CKD-treated kaolinite samples. For the second set of samples, kaolinite clay was treated with 25% (by weight of the

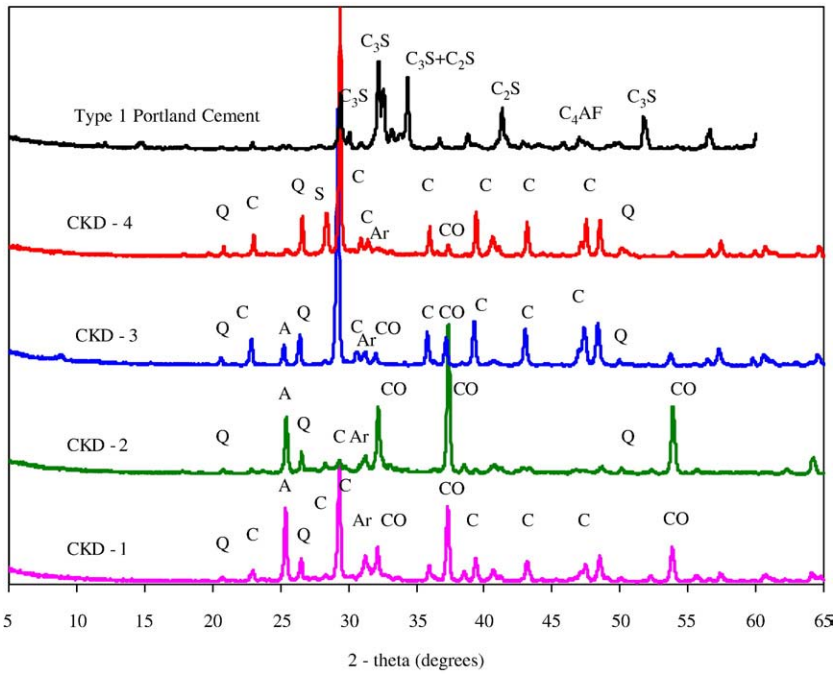

Fig. 2. X-ray patterns of CKD powders (Q–quartz, A–anhydrite, C–calcite, S–sylvite, Ar–arcanite, CO-free-lime (calcium oxide)).

clay) of each of the CKDs. The unconfined compressive strengths of hydrated CKD by themselves as well as that of the CKD-treated kaolinite samples were determined after 1, 7, 28 and 90 days of curing (same curing procedure as described in Section 3.1 was used). For each case, three replicate specimens were tested as per the procedures described in ASTM D 2166 [26] and the calculated average of the results was used in the analysis. The compressive strength test was performed using a universal testing machine operated in the displacement controlled mode at a strain rate of 1% per minute.

4. Results and discussion

4.1. X-ray analyses

The oxides in the CKDs may exist in various mineralogical phases, with the reactivity of these phases being significantly different. The mineral phases present in the CKDs determined by X-ray diffraction (XRD) for the individual CKDs are shown in Fig. 2. In all four CKDs considered in this study, the analytical CaO as reported in Table 2 actually existed in three different compounds: $CaCO_3$ (calcite), $CaSO_4$ (anhydrite), and free CaO (free-lime). The major mineral phases present in CKD-1 and CKD-2 were free-lime (CaO) and anhydrite ($CaSO_4$). The highest peak for the free-lime was observed in CKD-2, which corresponds to the highest value (~29%) determined by chemical analysis (Table 2). The second highest peak was observed in CKD-1 (~14% analytical free-lime). In addition, a significant amount of calcite ($CaCO_3$) was also present in CKD-1. The free-lime peaks for the remaining two CKDs were relatively low, again corresponding well to the analytical values of ~5% for CKD-3 and ~3% for CKD-4 shown in Table 2. The XRD patterns for these CKDs were dominated by the calcite peaks. Presence of quartz (SiO_2) and arcanite (K_2SO_4) was identified in all four CKDs but sylvite (KCl) was identified only in CKD-4.

The type and the amount of hydration products formed during reaction of CKDs with water (such as calcium hydroxide, ettringite, gypsum etc.,) play a major role in determining CKDs' effectiveness as soil stabilizers. Fig. 3 shows the X-ray diffraction pattern obtained for the hydrated CKDs after 1, 7, and 28 days of curing. Both of the high free-

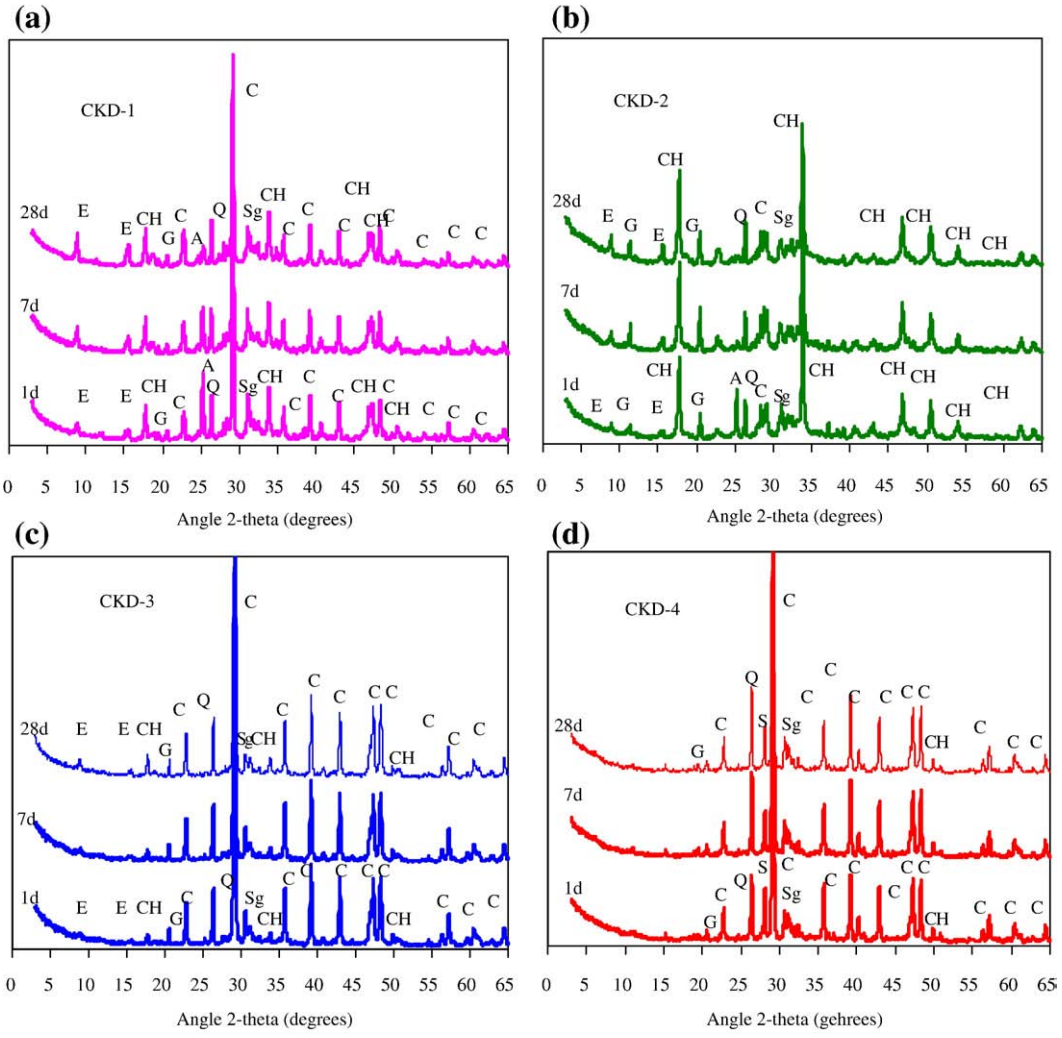

Fig. 3. X-ray patterns of hydrated CKDs specimens cured for 1, 7, and 28 days: (a) CKD-1, (b) CKD-2, (c) CKD-3, (d) CKD-4 (E–ettringite, CH–calcium hydroxide, G–gypsum, A–anhydrite, Q–quartz, C–calcite, S–sylvite, Sg–syngenite).

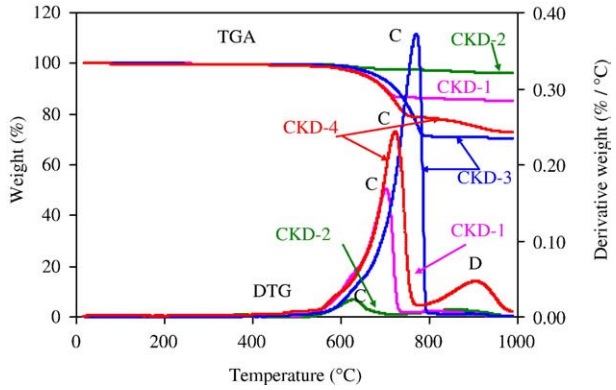

Fig. 4. Thermogravimetric analysis of CKD powder samples (C-calcite ($CaCO_3$), D-chloro silicate of calcium $Ca_3[SiO4]Cl_2$.

lime content CKDs (CKD-1 and CKD-2) produced significant amounts of calcium hydroxide (CH), ettringite (E) and syngenite (Sg) after water was added. In addition to these phases, a significant amount of gypsum was found in the hydrated CKD-2 after 1 day of hydration. The amount of gypsum increased upon further hydration (up to 7 days) but remained unchanged after that. Only traces of gypsum were found in CKD-1. In both of the high free-lime CKDs, the anhydrite present in the powder sample remained in the 1 day old hydrated specimen. However, its amount gradually decreased with increased curing period and almost all anhydrite disappeared by 28 days. It also appears that all free-lime present in the CKDs was converted to calcium hydroxide (CH) shortly after water was added since the amount of CH remained almost the same, irrespective of length of the curing period. The crystalline alkali sulfates phases, such as arcanites (K_2SO_4), present in dry CKDs were not retained in the wet-cured products, indicating the high solubility of these materials.

In the case of low free-lime content CKDs (CKD-3 and CKD-4), relatively small amounts of ettringites and calcium hydroxides were formed. The height of the XRD peak for the sylvite (KCl) compound found in dry CKD-4 decreased slightly due to the addition of water and further curing. The dominating calcite peaks and the quartz peaks present in these CKD powders remained unchanged in the wet-cured CKDs, indicating the inert nature of these two compounds.

4.2. Thermogravimetric analyses

Fig. 4 shows the TGA and (DTG) patterns obtained for all four CKD powders. None of the CKDs experienced any significant weight change in the temperature range of 0 to 550 °C, but a significant weight loss was observed in the temperature range of 600 to 800 °C, which indicates the

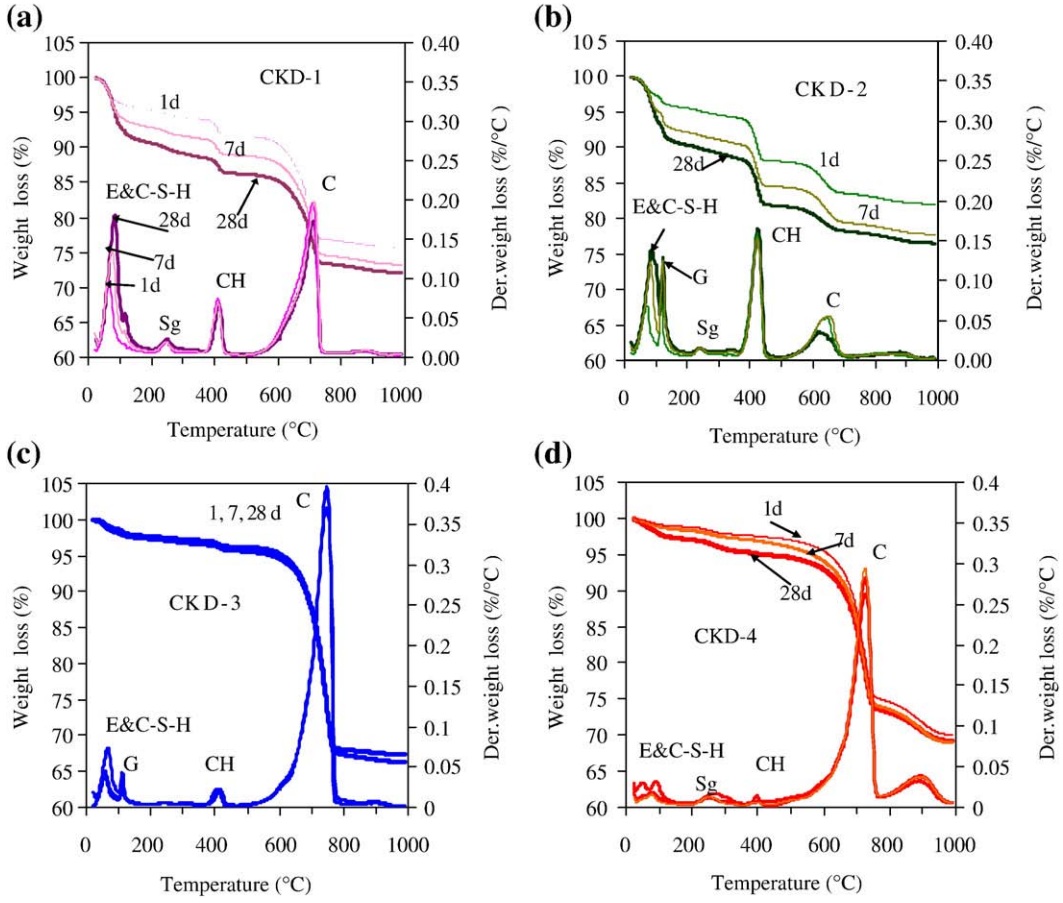

Fig. 5. Thermogravimetric analysis of CKDs samples hydrated for 1,7,and 28 days: (a) CKD-1, (b) CKD-2, (c) CKD-3, (d) CKD-4 (E–ettringite, C-S-H–calcium silicate hydrate,, G–gypsum, Sg–syngenite, CH–calcium hydroxide, C–calcite).

removal of CO_2 during the conversion of $CaCO_3$ to CaO. In addition to this, CKD-4 experienced a secondary weight loss centered around a temperature of 915 °C. Since CKD-4 had significantly higher chloride content compared to the rest of the CKDs, this peak could be due to the decomposition of chloride silicate of calcium, $Ca_3[SiO_4]Cl_2$. From the TGA analyses, the amount of $CaCO_3$ present in each CKD was calculated as approximately 30, 7, 64 and 58% in CKD-1, 2, 3 and 4, respectively. This agrees well with the results of XRD and the chemical analyses.

Fig. 5(a) and (b) show the thermal response (weight loss) of hydrated high free-lime content CKDs, after 1, 7 and 28 days of curing. The weight loss that happened at 70–100 °C was primarily caused by loss of water from the ettringite (E) crystals and calcium silicate hydrate (C-S-H) during their thermal decompositions. The possible presence of C-S-H, despite the absence of alite/belite in the XRD analyses needs further explanation. Compared to the amount of 10 to 16% of SiO_2 (chemical analysis shown in Table 2), relatively smaller amount of quartz (approximately 5%) was observed by XRD analyses.

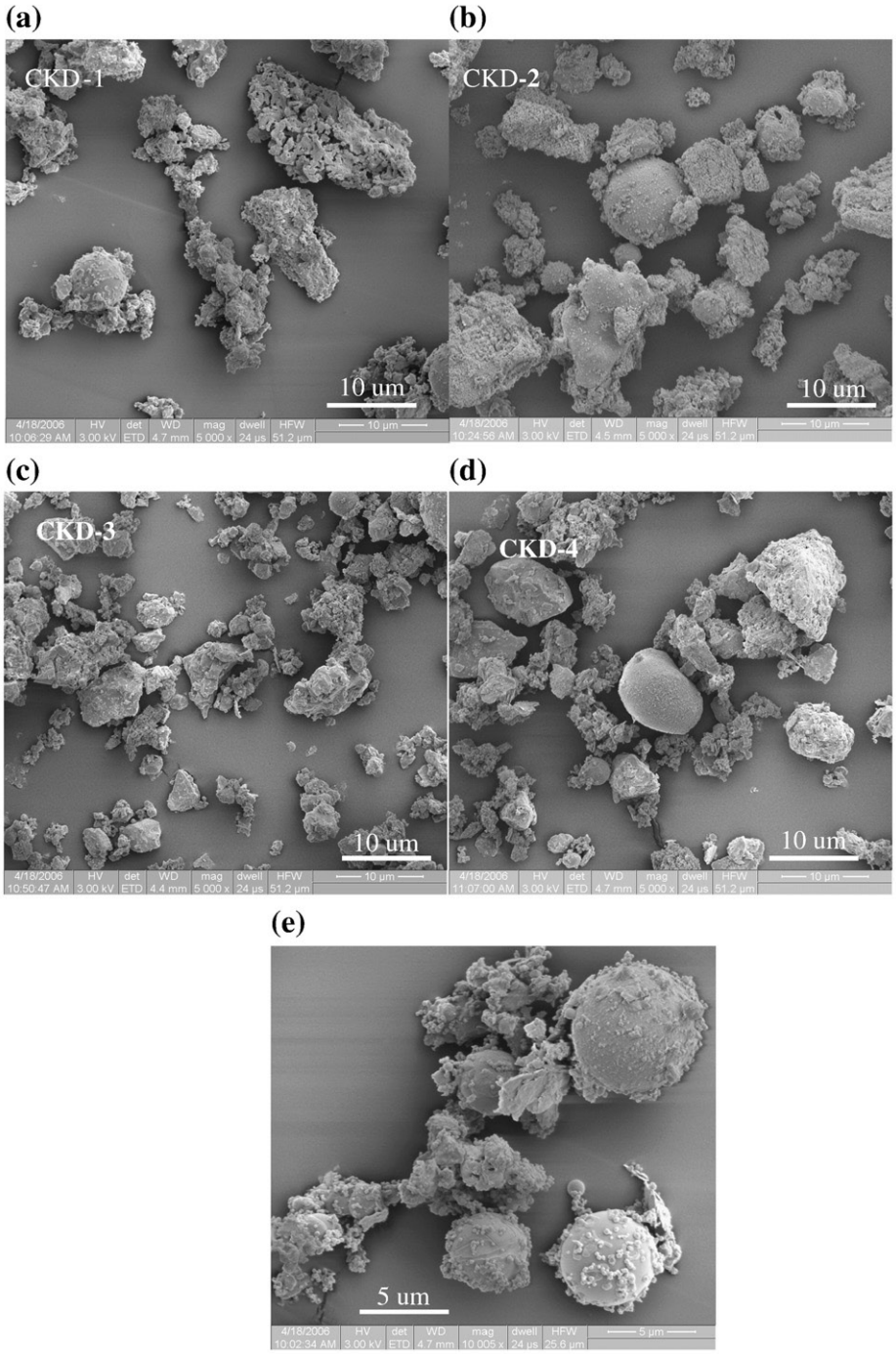

Fig. 6. Scanning electron micrographs of CKD powders: (a) CKD-1, (b) CKD-2, (c) CKD-3, (d) CKD-4, (e) close up-of the cluster containing both the agglomerated and spherical particles covered with very fine deposits in CKD-1.

This implies that the rest of the SiO_2 might be present in the amorphous form as part of the fly-ash particles (presence of fly-ash particles were later confirmed by SEM analysis). The amorphous SiO_2 might also be derived from dehydroxilated clay used as a raw feed in the cement kiln. The amorphous silica might have reacted with calcium hydroxide to form C-S-H. The presence of other hydration products such as calcium hydroxide (430 °C), gypsum (125 °C), syngenite (250 °C) at all ages were also confirmed. The presence of calcite (650 °C) was also verified.

For the CKDs with low free-lime contents (CKD-3 and CKD-4) the peaks corresponding to ettringite, C-S-H, gypsum, syngenite and calcium hydroxide decompositions were very small, indicating the near-absence of these products of hydration. Again, for these two CKDs the results obtained by TGA were also consistent with the XRD results and showed dominating calcite peaks (approximately at 650 °C).

4.3. Morphology by scanning electron microscopy

The microscopic appearance of the CKD powders examined by SEM is shown in Fig. 6. In general, all of the CKDs were predominantly composed of clusters (agglomerates) of particles with poorly defined shapes. However, each CKD also contained some spherical fly ash particles. Large number of very fine deposits (Fig. 6(e)) covered the surfaces of some of the spherical particles, while other particles retained very smooth surface texture. The EDX spectrum collected from such particles had peaks for Al, Si, K, O and S. The EDX analyses also revealed the presence of calcite, quartz and anhydrite in all CKDs. Fig. 6 also gives an indication of the relative particle sizes in the agglomerates of each CKD.

Fig. 7 shows representative SEM micrographs of two hydrated CKDs (CKD-1 and CKD-2) taken at two different magnifications after a hydration period of 28 days. The particles' morphology was substantially altered from that of the unhydrated CKDs (shown in Fig. 6). All spherical particles originally present in the CKD powder disappeared and new products were formed. One of the prominent features of the microstructure of the hydrated CKD-1 and CKD-2 (high free-lime content CKDs) was the presence of orthorhombic, lath shaped particles, which were identified (by EDX analysis) as syngenite ($K_2.Ca(SO_4)_2.2H2O$), and are marked as "S" in these micrographs. The syngenite particles were present in various sizes, and had a smooth surface texture. The other features present in the hydrated microstructure of CKD-2 material (refer to Fig. 8) were large hexagonal calcium hydroxide crystals, and ettringite needles. Much of the fractured surface shows

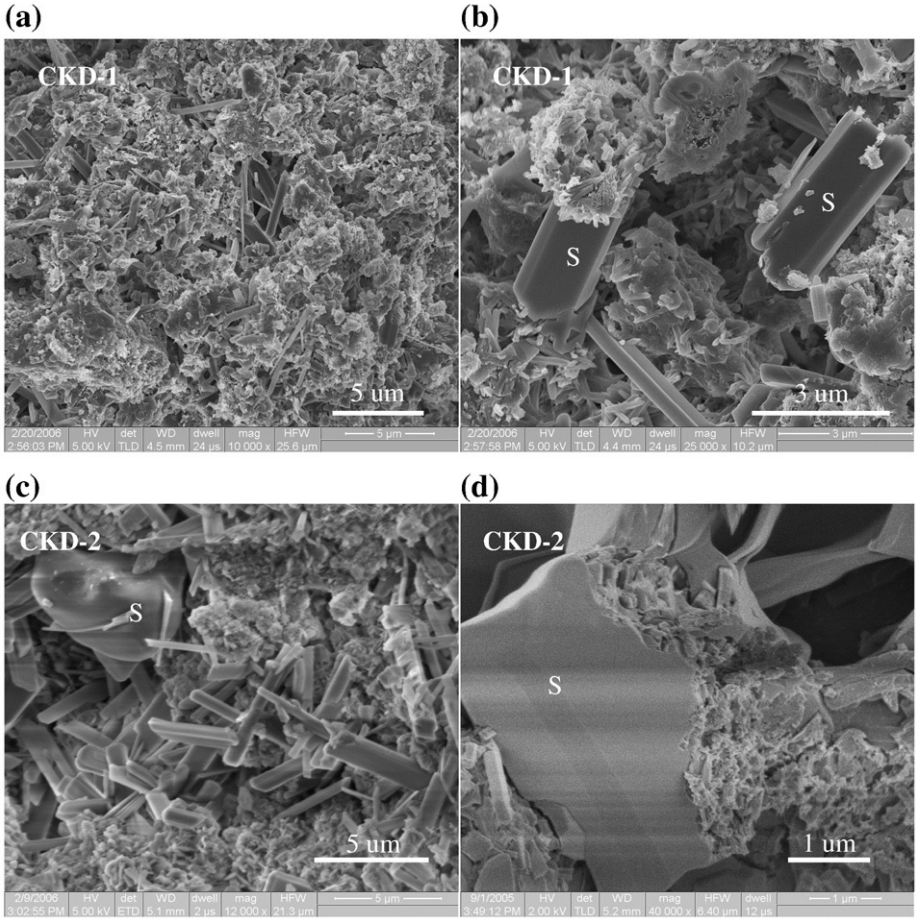

Fig. 7. Scanning electron micrographs of 28 days old hydrated CKD-1 and CKD-2 pastes (a) CKD-1 at low magnification, (b) CKD-1 at high magnification, (c) CKD-2 at low magnification, (d) CKD-2 at high magnification (S–syngenite,).

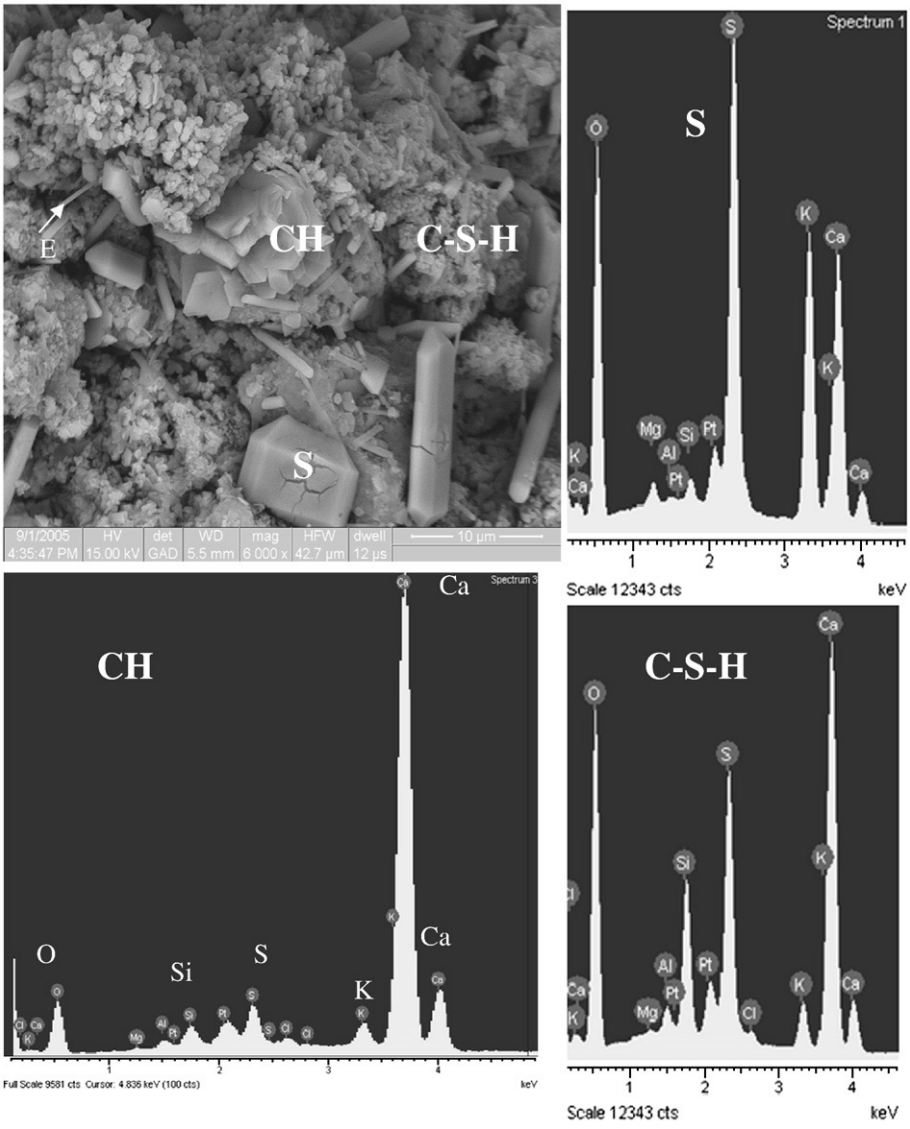

Fig. 8. SEM micrograph of hydrated CKD-2 (28 days old) showing syngenite (S), calcium hydroxide (CH), calcium silicate hydrate (C-S-H), and ettringite phases (E).

cemented fine particles containing calcium, silica, and sulfur and labeled as "C-S-H". These particles somewhat resemble calcium silicate hydrate in appearance, but incorporate significant amounts of sulfur and some potassium. No areas were found showing normal C-S-H spectra without significant amount of sulfur. Very similar features were also observed in the hydrated CKD-1 microstructure (not shown).

In the case of low free-lime CKDs (CKD-3 and CKD-4) neither the syngenite nor the calcium hydroxide crystals were found by SEM examination (Fig. 9). The main constituent of both these hydrated CKDs was the retained calcite, originally present in the CKD powder. The EDX spectrum collected from the C-S-H gel-like structure found in hydrated CKD-3 at few locations is shown in Fig. 9(e). However, the C-S-H gel-like morphology found in CKD-3 was entirely different from the morphology of the C-S-H like particles found in other CKDs, despite similarity of the EDX's spectra. Large numbers of potassium chloride crystals were also detected in CKD-4.

4.4. Unconfined compressive strength of compacted and hydrated CKD pastes

The strength development of hydrated CKD pastes was monitored over a period of 90 days (Fig. 10). After each of the curing periods, the highest compressive strength was achieved by the paste made from CKD-2, which, contained the highest amount of free-lime of all CKDs tested. Samples of CKD-2 cured for a period of 28 days achieved strength of approximately 5000 kPa and those cured for 90 days achieved 9000 kPa. CKD-1, which also had a relatively high amount of free-lime, achieved almost the same strength as CKD-2 at 28 days. However, little additional strength increase was observed for this CKD upon extended curing, and its 90 day strength was only 5500 kPa. CKDs with low free-lime content, CKD-3 and CKD-4, achieved strength of 3000 and 1500 kPa, respectively, for a curing period of 28 days.

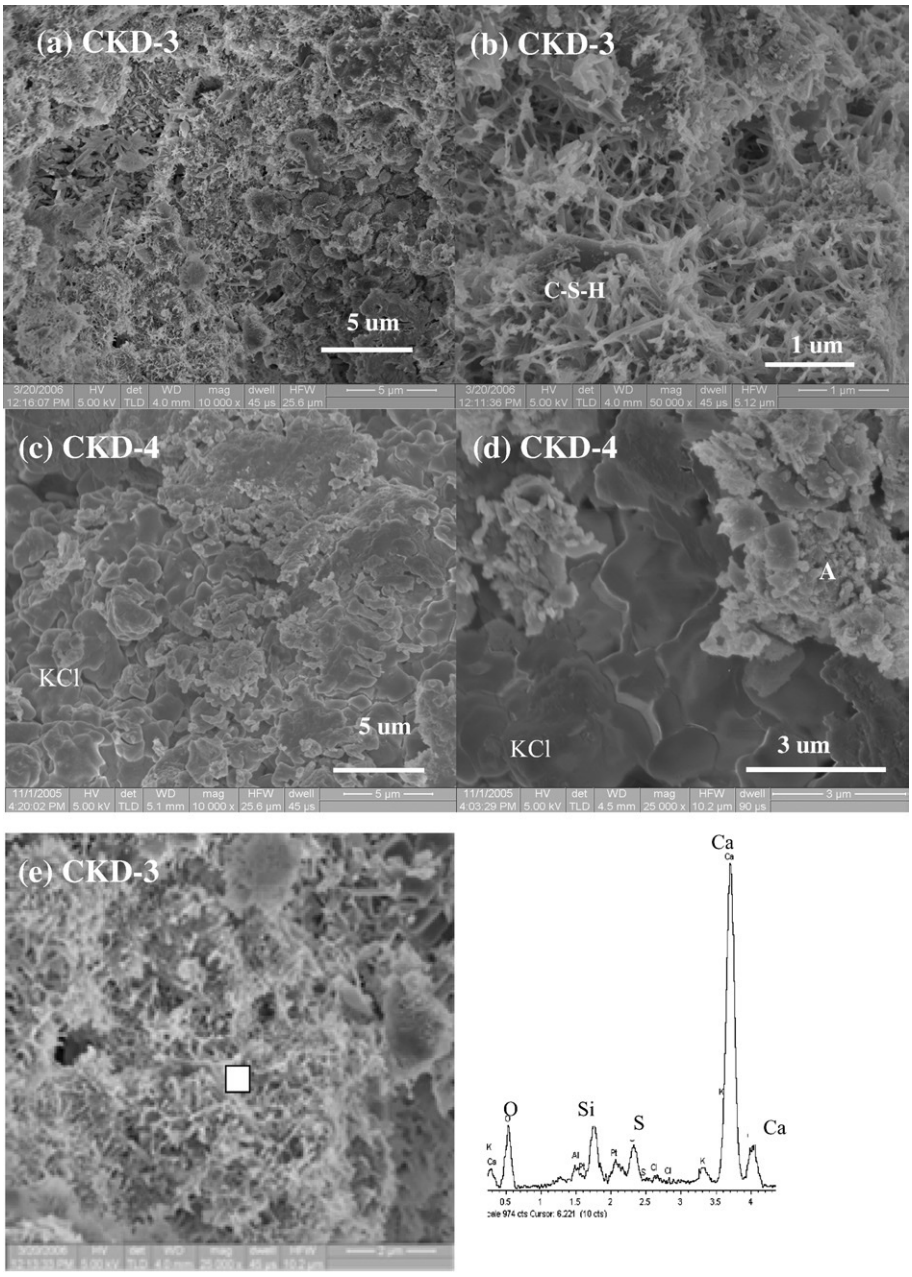

Fig. 9. Scanning electron micrographs of 28 days old hydrated CKD-3 and CKD-4 pastes (a) CKD-3 at low magnification, (b) CKD-3 at high magnification, (c) CKD-4 at low magnification, (d) CKD-4 at high magnification (e) EDX analysis of hydrated CKD-3 (C-S-H-calcium silicate hydrate, KCL–potassium chloride).

These results show that the CKDs with high free-lime contents, CKD-1 and CKD-2, showed better performance, in terms of strength development. In addition to the self cementing nature of high free lime content CKDs, the ettringite, gypsum, syngenite along with some secondary C-S-H like phases identified in the microstructure of these CKDs may have contributed to the observed strength development. However, it should be noted that ettringite (and other sulfate bearing phases) may be detrimental to the long term durability of stabilized soil. The amounts of these hydration products were much lower in the hydrated low-free-lime content CKDs and hence, the strength of CKD-3 and 4 were relatively lower. Although, some C-S-H gel-like phases were present in the microstructure of CKD-3, they did not appear to have influenced the strength development.

The relative performance of CKDs can also be affected by their physical properties. This can be confirmed by observing the strength development of high free-lime content CKD-1 and CKD-2. Though these two CKDs have large difference, in free-lime contents, which is probably the most important parameter contributing to the strength, both showed similar patterns of strength development up to 28 days. The CKD-1, which had only ~14% free-lime content, compared to ~29% in CKD-2, was much finer than the latter. The increase in fineness, which increases the reactivity, could be the reason for similar performance of CKD-1 compared to that of CKD-2, despite

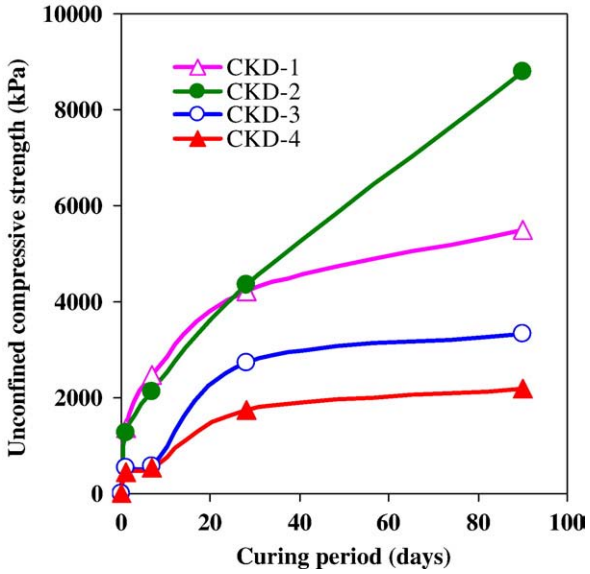

Fig. 10. Unconfined compressive strength of the hydrated CKD pastes (water content—31%).

lower free-lime content of the former. The lower strength at 90 day curing period for CKD-1 compared to CKD-2 could be due to several other factors. For example, the relatively higher percentage of SiO_2 in CKD-2 might have resulted in continued formation of C-S-H in that material compared to CKD-1.

4.5. Unconfined compressive strength of compacted and hydrated CKD-treated kaolinite clay

The unconfined compressive strength (UCS) of kaolinite clay treated with 25% (by weight of the clay) of various CKDs was monitored for up to 90 days and the results are shown in Fig. 11. This figure also shows the compacted strength of untreated clay cured for the same time periods. In all cases, the strengths of the CKD-treated clays were much higher than that of the untreated clay. The strengths of the high free-lime content CKD-treated kaolinite increased significantly compared to low-lime content CKD-treated clay. The increase in the UCS of the CKD- 1 treated samples beyond 28 days of curing period was limited; in contrast, the UCS of the CKD-2 treated and compacted clay kept increasing beyond 28 day curing period. The similar initial (up to 28 days) rate of strength development of CKD-1 treated kaolinite clay compared to CKD-2 treated kaolinite clay, despite low free-lime content of CKD-1, can be attributed to higher fineness and surface area of CKD-1. A very similar behavior was observed in the UCS of CKD pastes earlier, and again it would be due to difference in

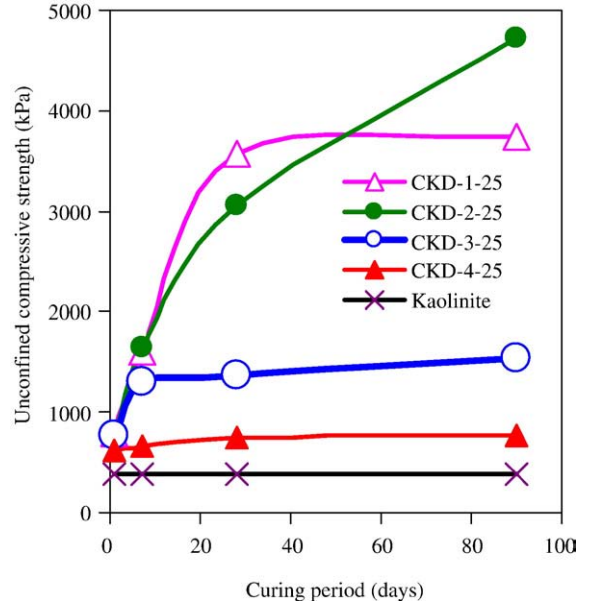

Fig. 11. Unconfined compressive strength of 25% CKD-treated kaolinite (water content—31%).

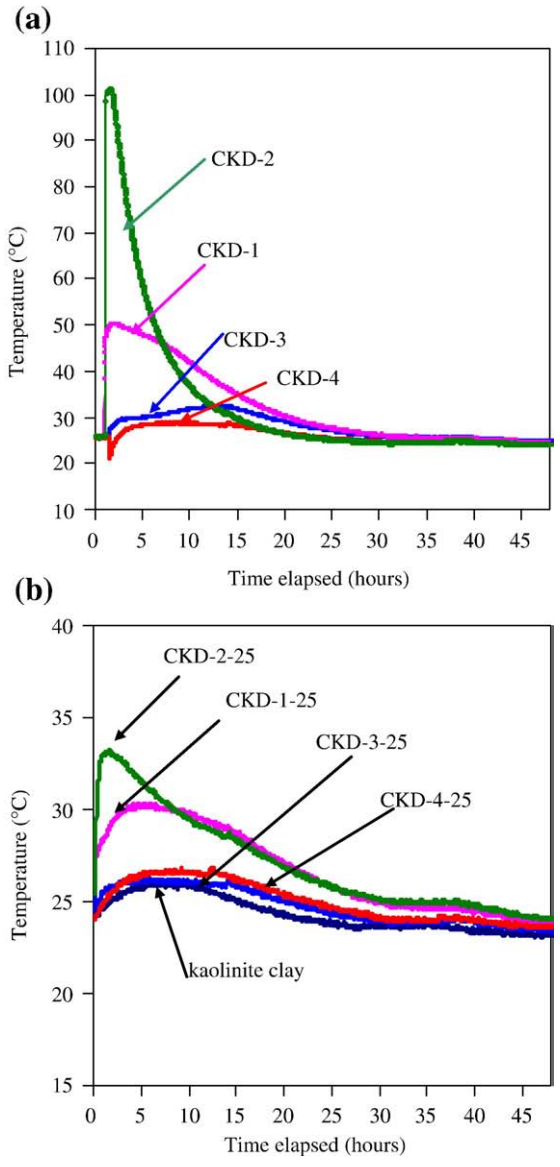

Fig. 12. Adiabatic temperature evolution during the hydration of (a) CKD pastes (b) 25% CKD-treated kaolinite (water content of 31%).

the fineness of these CKDs. Similar influence of free-lime content and fineness of CKD on the strength development of CKD-montmorillonite clay mixtures has been reported elsewhere [27]. A prolonged curing period did not have significant impact on the strength of CKD-3 and CKD-4 treated and compacted kaolinite clay. However, it should be noted that though these two CKDs were not as effective (in terms of improving the strength of the treated clay) as either CKD-1 or CKD-2, they could be still classified as effective stabilizer for this particular clay. As per ASTM D 4609, a material could be qualified as an effective stabilizer if it could increase the UCS of the soil by 350 kPa [28]. As expected, trends in strength development are very similar to those observed previously for compacted and hydrated CKD-alone paste samples (Fig. 10). Hence, the strength of the hydrated CKD paste may alone be used as an indicator of a potential of a particular CKD to be an effective clay soil stabilizer.

4.6. Temperature of hydration of CKD pastes

Temperature of hydration curves for each of the four CKDs hydrated with a water content of 31% is shown in the Fig. 12(a). After mixing with water, the CKD-1 and CKD-2 exhibited peak temperatures of approximately 50 °C and 100 °C, respectively. This was primarily due to the reaction of free-lime with water to form calcium hydroxide, which is an exothermic reaction. In the case of CKDs with relatively low amounts of free-lime (CKD-3 and CKD-4), the heat produced was significantly lower. Based on the heat generated, CKD-2 can be classified as highly reactive followed by CKD-1, CKD-3 and CKD-4, in that order. It can be seen (Fig. 11) that the CKDs with higher temperature of hydration were much more effective in increasing the strength of the kaolinite clay at any given period of curing. It appears that the temperature of hydration of CKD paste may also be taken as another indicator of the suitability of a CKD for soil stabilization.

It is also important to have an understanding of the approximate increase in temperature of the soil due to CKD treatment because of the following reasons (1) safety of the workers and (2) the increase in temperature may cause the drying of the wet cohesive soils easily and thus may increase their workability. The temperature of hydration of CKD-treated kaolinite clay was also measured in a similar fashion as that of the hydrated CKD paste and is presented in Fig. 12(b). The temperature of neat kaolinite clay paste remained constant during the entire period of measurement at 25 °C. The addition of 25% of CKD-1, 2, 3, and 4 caused respectively, 5, 8, 1 and 1 °C rise in the hydration temperature of the clay-CKD mixtures. This moderate increase in temperature should not cause any safety problems and may be helpful when stabilizing wet cohesive soils especially in the case of CKD-1 and CKD-2.

5. Summary

The important conclusions of the present study are summarized as follows:

- Significant amounts of calcium hydroxide, syngenite and ettringite were identified in hydrated high free-lime content CKDs. These products were either absent or present only in much smaller quantities in hydrated low free-lime content CKDs.
- In high free-lime content CKDs the amount of ettringite increased with the increased curing period.
- When hydrated, CKDs with high free-lime content exhibited higher strength compared to low free-lime content CKDs. This may be attributed to the formation of increased amounts of ettringite and secondary C-S-H during hydration of these CKDs.
- Apart from free-lime content, fineness of CKDs also influenced the strength development, especially at early ages.
- CKD with high free-lime content exhibited higher temperature of hydration compared to low free-lime content CKDs.
- Both compressive strength of hydrated CKD paste and the temperature of hydration itself provide good indication of the performance of these CKDs when used as soil stabilizers.
- As expected, high free-lime content CKDs significantly enhanced the unconfined compressive strength of the kaolinite clay compared to the low free lime content CKDs. Although not as effective as CKDs with high free-lime content, they were, nevertheless capable of increasing the strength of the kaolinite clay from 100 to 300% after 7 days of curing. Hence these CKDs may also be qualified as potential stabilizers for kaolinite clays.

References

[1] U.S. Department of Transportation (USDOT) Federal Highway Administration: Turner Fairbanks Highway Research Center, User guidelines for waste and by-product materials in pavement construction: FHWA-RD-97-148 April 1998, 1998.
[2] J.R. Connor, S. Cotton, P.P. Lear, Chemical stabilization of contaminated soils and sludges using cement and cement by products, Proceedings of the Cement Industry Solutions to Waste Management, Calgary, Alberta, Canada, Oct. 7–9 1992, pp. 73–97.
[3] M. McKay, J. Emery, Stabilization/solidification of contaminated soils and sludges using cementitious systems, Proceedings of the Cement Industry Solutions to Waste Management, Calgary, Alberta, Canada, Oct. 7–9 1992, pp. 135–151.
[4] M.S.Y. Bhatty, Properties of blended cement made with portland cement, cement kiln dust, fly ash and slag, Proceedings of the 8th International Congress on the Chemistry of Cement, Rio de Janeiro, Brazil, Sept. 22–28 1986, pp. 118–127.
[5] M.L. Wang, V. Ramakrishnan, Evaluation of blended cement, mortar and concrete made from type III cement and kiln dust, Construction and Building Materials 4 (2) (1990) 78–97.
[6] R.J. Detwiler, J.I. Bhatty, S. Bhattacharja, Supplementary cementitious materials for use in blended cements, R&D Bulletin, vol. 112, Portland Cement Association, Skokie, Illinois, 1996.
[7] F.F. Udoeyo, A. Hyee, Strength of cement kiln dust concrete, ASCE Journal of Materials in Civil Engineering 14 (96) (2002) 524–526.
[8] A.S. Al-Harthy, R. Taha, F. Al-Maamary, Effect of cement kiln dust (CKD) on mortar and concrete mixtures, Construction and Building Materials, 17 (2003) 353–360.
[9] M.S. Konsta-Gdoutos, S.P. Shah, Synthesis and properties of novel blended cements based on CKD-Slag blends, Cement and Concrete Research 33 (2003) 269–276.

[10] K. Wang, M.S. Konsta-Gdoutos, S.P. Shah, Hydration, rheology and strength of OPC-CKD-Slag binders, ACI Materials Journal 99 (2) (2002) 173–179.
[11] G.J. Hawkins, J.I. Bhatty, A.T. O'Hare, Cement Kiln Dust Production, Management and Disposal, R&D Serial No.2327, Portland Cement Association, Skokie, Illinois, 2003.
[12] G. Ballivy, J. Rouis, D. Breton, Use of cement residual kiln dust as landfill liner, Proceedings of the Cement Industry Solutions to Waste Management, Calgary, Alberta, Canada, Oct. 7–9 1992, pp. 99–118.
[13] M.L. Preston, Use of cement kiln dust as an agricultural lime and fertilizer, Emerging Technologies Symposium on Cement and Concrete in the Global Environment, Chicago, PCA's Cement Technical Support Library DVD020.01©2005, Portland Cement Association, Skokie, Illinois, March 10–11 1993.
[14] C.E. Pierce, H. Tripathi, T.W. Brown, Cement kiln dust in controlled low-strength materials, ACI Materials Journal 100 (6) (2003) 455–462.
[15] A. Katz, K. Kovler, Utilization of industrial by product for the production of controlled low strength materials (CLSM), Waste Management 24 (2004) 501–512.
[16] J.I. Bhatty, Alternative Uses of Cement Kiln Dust, R&D Bulletin, vol. 327, Portland Cement Association, Skokie, Illinois, 1995.
[17] M.C. Santagata, A. Bobet, The Use of Cement Kiln Dust (CKD) for Subgrade Stabilization/Modification, SPR No. 2575, Purdue University, West Lafayette, Indiana, USA, 2002.
[18] G.A. Miller, S. Azad, Influence of soil type on stabilization with cement kiln dust, Construction and Building Materials 14 (2) (2000) 89–97.
[19] S. Peethamparan, J. Olek, K.E. Helfrich, Evaluation of the engineering properties of cement kiln dust (CKD) modified kaolinite clay, Proceedings of the 21st International Conference on Solid Waste Technology and Management, March 26–29, Widener University, Philadelphia, PA, 2006, pp. 997–1006.
[20] Z.A. Baghdadi, Utilization of kiln dust in clay stabilization, Journal of King Abdulaziz University: Engineering and Science 2 (1990) 153–163.
[21] Z.A. Baghdadi, M.A. Rahman, Potential of cement kiln dust for the stabilization of dune sand in highway construction, Building and Environment 25 (4) (1990) 285–289.
[22] S. Diamond, E.B. Kinter, Mechanism of soil-lime stabilization, an interpretive review, Highway Research Record 92 (1965) 83–96.
[23] J.R. Prusinski, S. Bhattacharja, Effectiveness of portland cement and lime in stabilizing clay soils, Transportation Research Record 1652 (1999) 215–227.
[24] USBR-5510, Procedure for performing laboratory compaction of soils—Harvard miniature, United States Department of the Interior, Bureau of Reclamation, Denver, Colorado, 1989.
[25] ASTM C150, Standard specification for portland cement, ASTM International, West Conshohocken, PA, 2001.
[26] ASTM D 2166, Standard test methods for unconfined compressive strength of cohesive soils, ASTM International, West Conshohocken, PA, 2000.
[27] S. Peethamparan, J. Olek, A study on the effectiveness of cement kiln dusts (CKDs) in stabilizing Na-montmorillonite clay, ASCE Journal of Materials in Civil Engineering 20 (2) (2008) 137–146.
[28] ASTM D 4609, Standard Guide for Evaluating Effectiveness of Admixtures for Soil Stabilization, ASTM International, West Conshohocken, PA, 2001.